

Electronic and Optical Properties of Energetic Particle-Irradiated In-rich InGaN

S.X. Li,^{1,2} K.M. Yu,¹ R.E. Jones,^{1,2} J. Wu,¹ W. Walukiewicz,¹ J.W. Ager III,¹ W. Shan,¹ E.E. Haller,^{1,2} Hai Lu,³ William J. Schaff,³ and W. Kemp⁴

¹ Materials Sciences Division, Lawrence Berkeley National Laboratory, Berkeley, CA 94720

² Department of Materials Science and Engineering, University of California, Berkeley, Berkeley, CA 94720

³ Department of Electrical and Computer Engineering, Cornell University, Ithaca, NY 14853

⁴ Air Force Research Laboratory, Kirtland Air Force Base, Kirtland AFB, NM 87117

ABSTRACT

We have carried out a systematic study of the effects of irradiation on the electronic and optical properties of InGaN alloys over the entire composition range. High energy electrons, protons, and $^4\text{He}^+$ were used to produce displacement damage doses (D_d) spanning over five orders of magnitude. The free electron concentrations in InN and In-rich InGaN increase with D_d and finally saturate after a sufficiently high D_d . The saturation of carrier density is attributed to the formation of native donors and the Fermi level pinning at the Fermi Stabilization Energy (E_{FS}), as predicted by the amphoteric native defect model. Electrochemical capacitance-voltage (ECV) measurements reveal a surface electron accumulation whose concentration is determined by pinning at E_{FS} .

INTRODUCTION

Among the group III-nitrides, InN, a narrow bandgap semiconductor [1, 2], is certainly the least studied. Even basic parameters, such as its direct bandgap value, were the subject of some controversy [3-8], it is now clear that InN a direct gap of of $\sim 0.7\text{eV}$, in contrast to the previously believed 1.9eV . In many instances the larger reported bandgap values can be understood by a significant Burstein-Moss shift due to the high free electron concentration in the samples [9]. The narrow bandgap of InN has opened up many new possible applications, such as InGaN tandem solar cells, inspired from the almost perfect match of InGaN bandgap span with the solar spectrum [10]. To test the irradiation hardness of InGaN, we have carried out a systematic study of the effects of irradiation on the electronic and optical properties of InGaN alloys over the entire composition range from InN to GaN. The irradiation, which produces mostly native point defects, also reveals the origin of the tendency of InN to be n-type, as predicted by the amphoteric defect model [11, 12].

EXPERIMENTAL DETAILS

The epitaxial InN and $\text{In}_{1-x}\text{Ga}_x\text{N}$ thin films (310-2700 nm thick) used in this study were grown on c-sapphire substrates by molecular beam epitaxy (MBE) with GaN as the buffer layer [13]. The initial free electron concentrations in these samples range from the low 10^{18} cm^{-3} to low 10^{17} cm^{-3} and the mobility ranged from $7\text{ cm}^2/\text{V}\cdot\text{s}$ ($x = 0.76$) to above $1500\text{ cm}^2/\text{Vs}$ ($x = 0$). In addition, a GaN sample ($3\text{ }\mu\text{m}$ thick with an electron concentration $\sim 7.74 \times 10^{17}\text{ cm}^{-3}$) and a

GaAs sample ($\sim 10\mu\text{m}$ thick with an electron concentration $\sim 8 \times 10^{16} \text{ cm}^{-3}$) were also included in this study.

The samples were irradiated with 1 MeV electrons, 2 MeV protons, and 2 MeV $^4\text{He}^+$ ions. The fluences of electrons ranged from 5×10^{15} to $1 \times 10^{17} \text{ cm}^{-2}$ and those of protons and $^4\text{He}^+$ from 1.12×10^{14} to $2.68 \times 10^{16} \text{ cm}^{-2}$. In all cases, the particle penetration depth greatly exceeded the film thickness, assuring a homogeneous damage distribution in the film. Ion channeling spectroscopy showed that the minimum yield χ increased from 0.04 in an as-grown InN sample to merely 0.11 after $^4\text{He}^+$ irradiation with a dose of $1.8 \times 10^{16} \text{ cm}^{-2}$, indicating that the InN films remains single crystalline in spite of the high concentration of radiation-induced defects. X-ray diffraction analysis revealed that after the heaviest $^4\text{He}^+$ dose ($2.68 \times 10^{16} \text{ cm}^{-2}$) the lattice parameter of the film increased by 0.02 \AA (0.35%). Since extended crystalline defects such as dislocations and twins do not alter the lattice parameter of a crystal, we believe that point defects are responsible for the observed changes in electrical properties of the irradiated materials.

We used the displacement damage dose methodology developed by the Naval Research Laboratory for modeling solar cell degradation in space environments to scale the irradiation damage [14,15]. The displacement damage dose (D_d , in units of MeV/g) is defined as the product of the non-ionizing energy loss (NIEL) and the particle fluence. In this work, the NIEL was either obtained from the tables in Ref. 16 or from the SRIM (the stopping and range of ions in matter) program [16].

To eliminate effects from sample inhomogeneity and variations in the properties of metal contacts in the Hall measurements, the evaluation of the proton and $^4\text{He}^+$ irradiation damage was done sequentially at progressively higher radiation doses on the same samples. Near-surface carrier concentration profiles of InGaN were measured with the Electrochemical Capacitance-Voltage (ECV) technique with 0.2M NaOH: EDTA as the electrolyte.

RESULTS AND DISCUSSION

The free electron concentrations of InN, $\text{In}_{0.4}\text{Ga}_{0.6}\text{N}$, GaAs, and GaN are plotted against D_d in Fig. 1. Irradiation increases the free electron concentrations in InN and $\text{In}_{0.4}\text{Ga}_{0.6}\text{N}$, which eventually saturate at a value depending on the alloy composition as D_d exceeds 10^{16} MeV/g . The largest increase and highest saturation concentration are found in InN, where the electron concentration rises by a factor of about 300. In contrast, irradiation reduces the free electron concentrations in GaN and GaAs. At D_d higher than about 10^{13} MeV/g , the electron concentration in GaN decreases rapidly. The radiation-induced reduction of the free electron concentration in GaAs, which is a well-established observation, occurs at a

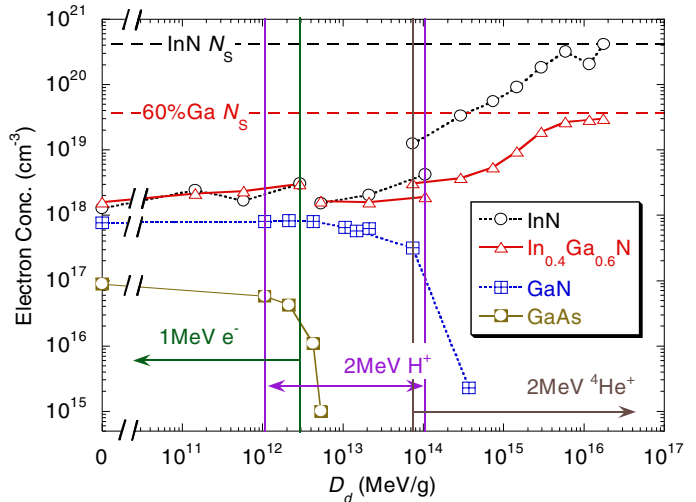


Figure 1. Electron concentrations in InN, $\text{In}_{0.4}\text{Ga}_{0.6}\text{N}$, GaN, and GaAs as function of D_d . The calculated N_s of InN and $\text{In}_{0.4}\text{Ga}_{0.6}\text{N}$ are also marked as dotted lines.

lower D_d of mid- 10^{12} MeV/g. It is important to note that although all three nitride samples had very similar starting electron concentrations, the irradiation had profoundly different effects on their properties. The observed increase of electron concentration in InN and $\text{In}_{0.4}\text{Ga}_{0.6}\text{N}$ shows that the damage creates donor-like defects. On the other hand, the reduction of the electron concentration in GaN and GaAs clearly demonstrates that acceptors are the dominant radiation-induced defects in these materials.

Our results can be readily understood using the amphoteric defect model [11,12], which predicts that the broken-bond type of defects have a universal energy level which is called Fermi level stabilization energy (E_{FS}). The point defects introduced by irradiation in our experiment all have their energy level at E_{FS} . Figure 2 shows the conduction band edge (CBE) and the valence band edge (VBE) energies relative to the vacuum level in $\text{In}_{1-x}\text{Ga}_x\text{N}$, GaAs and $\text{Ga}_{0.5}\text{In}_{0.5}\text{P}$ [10]. Both GaAs and $\text{Ga}_{0.5}\text{In}_{0.5}\text{P}$ are important materials in current state-of-the-art tandem solar cells. The position of E_{FS} at 4.9 eV below the vacuum level is also shown. It is important to note that the value of the electron affinity of InN (5.8 eV) is larger than that of any other semiconductor. This extremely low location of the CBE explains the n-type activity and the effect of defects on the properties of InN. Since E_{FS} is located high in the conduction band (~ 0.9 eV above the CBE), native donors are the dominant defects introduced by irradiation damage, and, at large doses, these defects push the Fermi energy (E_F) towards E_{FS} . When the damage is sufficiently high, the electron concentration saturates at a certain value (which we call N_S) as E_F reaches E_{FS} . At this point acceptor- and donor-like defects are incorporated at the same rate and compensate each other. As a consequence, the Fermi level is pinned at E_{FS} and does not change with further radiation damage. For $\text{In}_{1-x}\text{Ga}_x\text{N}$ alloys, as x increases (more Ga), the CBE moves closer to E_{FS} , which results in a lower value of N_S . In $\text{In}_{1-x}\text{Ga}_x\text{N}$ with a Ga fraction higher than 66%, E_{FS} falls below the CBE, i.e., inside the bandgap. In pure GaN, E_{FS} is located ~ 0.7 eV below the CBE; therefore, in an n-type sample E_F lies above E_{FS} and radiation-induced native defects have acceptor-like character and are expected to compensate the donors, reducing the electron concentration. This is indeed what is observed in Fig. 1 for GaN. The same effect is observed in n-type GaAs; in this case irradiation moves E_F into the lower half of the band gap, resulting in highly resistive material.

To quantify the effect of irradiation on the electron concentration, we calculated N_S using the following expression [17] for a nonparabolic conduction band with $E_F = E_{FS}$:

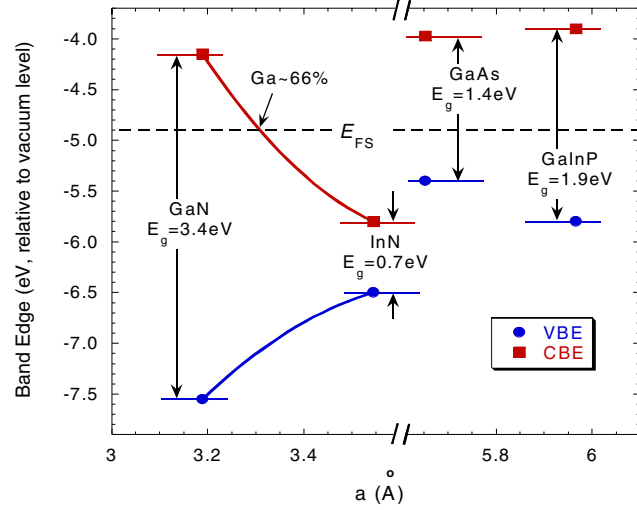


Figure 2. Positions of the valence band maxima and conduction band minima for InGaN alloys, GaAs, and $\text{Ga}_{0.5}\text{In}_{0.5}\text{P}$ [10]. The Fermi stabilization energy (E_{FS}) at $E_{vac} - 4.9$ eV is also shown.

$$N_s = \frac{1}{3\pi^2} \left(\frac{2m^*}{\hbar^2} \right)^{3/2} \int_{E_{CBE}}^{\infty} \frac{e^{\frac{E-E_{FS}}{k_B T}} [E - E_C + (E - E_C)^2 / E_g]^{3/2}}{[1 + e^{\frac{E-E_{FS}}{k_B T}}]^2} dE, \quad (1)$$

where m^* is the band edge effective electron mass, E_C is the energy of the CBE, and E_g is the bandgap. An additional important factor is the band-gap renormalization effect [18]. At sufficiently high electron concentrations electron-electron and electron-ion interactions can significantly reduce the fundamental bandgap. Here both effects contribute to the shift of the CBE whereas the energy of the defect level is affected only by the electron-ion interaction. Consequently the net shift of the CBE with respect to the localized defect level is given only by the electron-electron interaction.

N_s values of InN and $\text{In}_{0.4}\text{Ga}_{0.6}\text{N}$ calculated from Equation (1) are marked as dotted lines in Fig. 1. They are in good agreement with the observed saturation electron concentration. Calculated values of N_s are plotted as a function of alloy composition in Fig. 3. In the calculation, m^* is extrapolated linearly between InN and GaN and a bowing parameter of 1.43 eV is used to calculate the bandgap. The calculations are in excellent agreement with experimental N_s values obtained from a number of $\text{In}_{1-x}\text{Ga}_x\text{N}$ samples ($0 \leq x \leq 0.76$) after heavy irradiation ($D_d > 10^{16}$ MeV/g).

Our results show that, as predicted by the amphoteric defect model, incorporation of a high concentration of point defects stabilizes the Fermi energy at E_{FS} . It has been demonstrated before that the same effect is responsible for the pinning of the Fermi energy on semiconductor surfaces [11, 12]. To test this assertion we carried out measurements of the surface accumulation effect in InGaN alloys using a capacitance-voltage technique *<it would be ECV if we did etching>*. In this method a potential is applied across the electrolyte/semiconductor interface to probe the charge distribution below the semiconductor surface. A Helmholtz double layer, formed in the electrolyte, acts as an insulator whose capacitance can be changed by varying the applied bias [19]. Charge density can be obtained from the capacitance and applied bias [20]. The electron concentration profiles of a number of $\text{In}_{1-x}\text{Ga}_x\text{N}$ alloys and their endpoint compounds (InN and GaN) are shown in Fig. 4. For comparison the calculated N_s and bulk electron concentration measured by Hall effect are also shown. The profiles of the charge distribution in the samples with $x \leq 0.6$ clearly show an electron accumulation layer near the surface. For these samples, the carrier concentration decreases away from the surface and reaches its bulk value at the depth of few nm below the surface. The profiles also indicate that

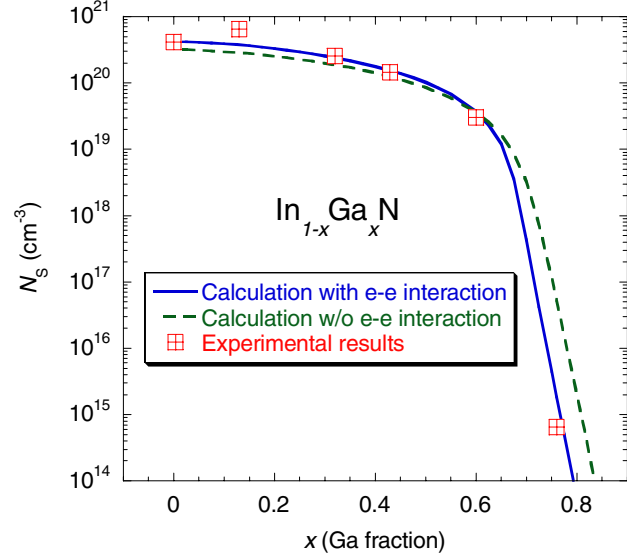


Figure 3. The calculated N_s (solid line) and experimental saturation electron concentrations (square dots) after heavy irradiation ($D_d > 10^{16}$ MeV/g) as function of alloy composition. A calculation performed without considering the electron-electron interaction is also shown (dotted line).

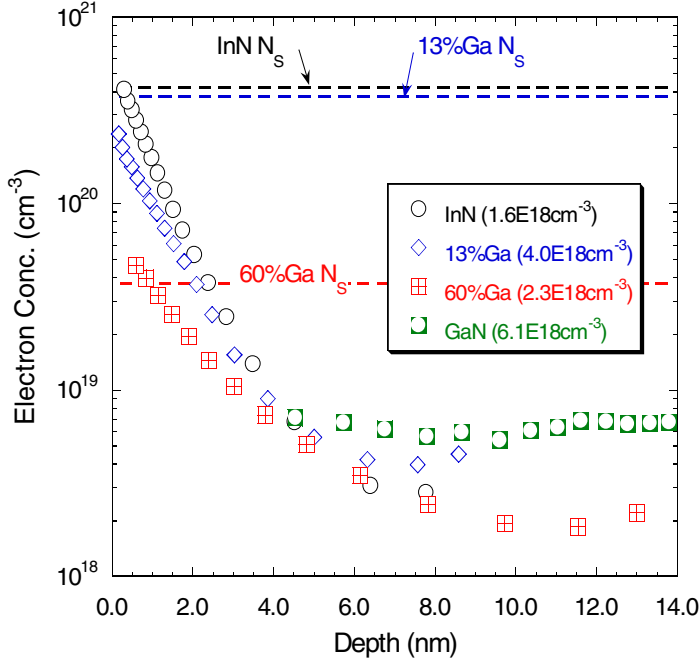


Figure 4. ECV measurements of the electron concentration depth profile in InGaN are plotted together with their corresponding N_S values. The bulk carrier concentrations, determined from Hall Effect, are shown in the legend.

the surface accumulation effect weakens as the Ga fraction increases. As seen in Fig. 4 there is no surface accumulation in GaN. This is consistent with well established fact that the surface Fermi energy is pinned in the band gap leading to surface electron depletion in this material [21].

The good agreement between the surface electron concentrations and the radiation damage-stabilized N_S indicates that in both cases the same, most likely vacancy-like, defects are responsible for the stabilization of the Fermi energy. This is the first experimental evidence that the amphoteric defect model, which has been successfully used to describe defect behavior in standard III-V semiconductors, is also applicable to group III-nitride alloys. Using known band edge alignments [22] we can position E_{FS}

in all group III-nitrides. For instance, in $\text{In}_{1-y}\text{Al}_y\text{N}$ alloys E_{FS} falls below CBE for $y > 0.29$, whereas at the AlN end point it is located 2.7 eV below CBE.

CONCLUSIONS

We have shown that the incorporation of high concentrations of native defects produced by high energy particle irradiation stabilizes the bulk Fermi energy in $\text{In}_{1-x}\text{Ga}_x\text{N}$ alloys. The stabilized energy is the same as the surface Fermi level pinning energy in In-rich $\text{In}_{1-x}\text{Ga}_x\text{N}$. Its position ranges from 0.9 eV above the CBE in InN to about 0.7 eV below the conduction band edge in GaN. The results confirm the applicability of the amphoteric defect model to the group III-nitride alloys.

ACKNOWLEDGEMENT

We thank L. Reichertz and B. Cardozo for providing the GaAs sample and Mr. Milton Yeh of Blue Photonics Inc. for the GaN sample. This work is supported by the Director's Innovation Initiative Program, National Reconnaissance Office and by the Director, Office of Science, Office of Basic Energy Sciences, Division of Materials Sciences and Engineering of the U.S. Department of Energy under Contract No. DE-AC03-76SF00098. The work at Cornell University is supported by ONR under Contract No. N000149910936.

REFERENCES

- [1] V. Yu. Davydov, A. A. Klochikhin, R. P. Seisyan, V. V. Emtsev, S. V. Ivanov, F. Bechstedt, J. Furthmüller, H. Harima, A. V. Mudryi, J. Aderhold, O. Semchinova, and J. Graul, *Phys. Status Solidi B* **229**, R1 (2002).
- [2] J. Wu, W. Walukiewicz, K.M. Yu, J.W. Ager III, E.E. Haller, H. Lu, W.J. Schaff, Y. Saito, Y. Nanishi, *Appl. Phys. Lett.* **80**, 3967 (2002).
- [3] Y. Nanishi, Y. Saito, and T. Yamaguchi, *Jap. J. Appl. Phys.* **42**, 2549 (2003).
- [4] Fei Chen, A.N. Cartwright, Hai Lu, and William J. Schaff, *J. Cryst. Growth*, **269**, 10 (2004).
- [5] R. Goldhahn, A. T. Winzer, V. Cimalla, O. Ambacher, C. Cobet, W. Richter, N. Esser, J. Furthmüller, F. Bechstedt, Hai Lu, and W. J. Schaff, *Superlattices and Microstructures*, **36**, 591 (2004).
- [6] O. Briot, B. Maleyre, S. Ruffenach, B. Gil, C. Pinquier, F. Demangeot, and J. Frandon, *J. Cryst. Growth*, **269**, 22 (2004).
- [7] T.V. Shubina, S.V. Ivanov, V. N. Jmerik, D. D. Solnyshkov, V. A. Vekshin, P. S. Kop'ev, A. Vasson, J. Leymarie, A. Kavokin, H. Amano, K. Shimono, A. Kasic, and B. Monemar, *Phys. Rev. Lett.* **92**, 117407 (2004).
- [8] K. M. Yu, Z. Liliental-Weber, W. Walukiewicz, S. X. Li, R. E. Jones, W. Shan, J. W. Ager III, E. E. Haller, Hai Lu, and William J. Schaff, *Appl. Phys. Lett.* **86**, 071910 (2005).
- [9] J. Wu, W. Walukiewicz, S. X. Li, R. Armitage, J. C. Ho, E. R. Weber, E. E. Haller, Hai Lu, William J. Schaff, A. Barcz, and R. Jakiela, *Appl. Phys. Lett.* **84**, 2805 (2004).
- [10] J. Wu, W. Walukiewicz, K. M. Yu, W. Shan, and J. W. Ager III, E. E. Haller, Hai Lu and William J. Schaff, W. K. Metzger, and Sarah Kurtz, *J. Appl. Phys.* **94**, 6477 (2003) and reference therein.
- [11] W. Walukiewicz, *Appl. Phys. Lett.* **54**, 2094 (1989).
- [12] W. Walukiewicz, *Physica B*, **302**, 123 (2001).
- [13] H. Lu, William J. Schaff, Jeonghyun Hwang, Hong Wu, Goutam Koley, and Lester E. Eastman, *Appl. Phys. Lett.* **79**, 1489 (2001).
- [14] S. R. Messenger, G. P. Summers, E. A. Burke, R. J. Walters, and M. A. Xapsos, *Progress in Photovoltaics: Research and Applications*, **9**, 103 (2001).
- [15] S. R. Messenger, E. A. Burke, G. P. Summers, M. A. Sapsos, R. J. Walters, E. M. Jackson, and B. D. Weaver, *IEEE Trans. Nuclear Sci.* **46**, 1595 (1999).
- [16] J. F. Ziegler, J. P. Biersack, and U. Littmark, *The Stopping and Range of Ions in Solids*, vol. 1 Pergamon Press, New York (1985).
- [17] W. Zawadzki and W. Szyamańska, *Phys. Stat. Sol.* **45**, 415 (1971).
- [18] J. Wu, W. Walukiewicz, W. Shan, K. M. Yu, J. W. Ager III, E. E. Haller, Hai Lu, and William J. Schaff, *Phys. Rev. B* **66**, 201403 (2002).
- [19] P. Blood, *Semicond. Sci. Tech.* **1**, 7 (1986).
- [20] William J. Schaff, Hai Lu, Lester F. Eastman, Wladek Walukiewicz, Kin Man Yu, Stacia Keller, Sarah Kurtz, Brian Keyes, and Lynn Ge, *ECS Fall 2004 Proceeding* (in press).
- [21] S. Arulkumaran, T. Egawa, G.-Y. Zhao, H. Ishikawa, T. Jimbo, and M. Umeno, *Jpn. J. Appl. Phys. Part 2*, **39**, L351 (2000).
- [22] J. Wu, W. Walukiewicz, K.M. Yu, J.W. Ager III, S.X. Li, E.E. Haller, Hai Lu, and William J. Schaff, *Solid State Communications* **127**, 411 (2003).